Stephen E. Harding*
University of Nottingham
Department of Applied
Biochemistry and Food Science
Sutton Bonington LE12 5RD,
United Kingdom

Gisela Berth
Norwegian Biopolymer
Laboratory (NOBIPOL)
Department of Biotechnology
University of Trondheim
NTH, N-7034, Norway

Jürgen Hartmann
Max-Planck-Institut for Colloid
and Interface Science
D-14513 Teltow, Germany

Kornelia Jumel
University of Nottingham
Department of Applied
Biochemistry and Food Science
Sutton Bonington LE12 5RD,
United Kingdom

Helmut Cölfen
University of Nottingham
Department of Applied
Biochemistry and Food Science
Sutton Bonington LE12 5RD,
United Kingdom

Bjørn E. Christensen
Norwegian Biopolymer
Laboratory (NOBIPOL)
Department of Biotechnology
University of Trondheim
NTH, N-7034, Norway

Physicochemical Studies on Xylinan (Acetan). III. Hydrodynamic Characterization by Analytical Ultracentrifugation and Dynamic Light Scattering

A laboratory-made sample of the polysaccharide xylinan (acetan) has been further characterized with respect to (i) purity, (ii) molar mass and polydispersity, and (iii) gross conformation by a combination of hydrodynamic measurements (sedimentation velocity and equilibrium analytical ultracentrifugation, viscometry, and dynamic light scattering) in aqueous NaCl ($I = 0.10\ mol \cdot L^{-1}$*). Sedimentation velocity diagrams recorded using Schlieren optics revealed highly pure material sedimenting as a single boundary [*$s^{\circ}_{20,w} = 9.5 \pm 0.7$*) S; $k_s = (273 \pm 112)$ mL/g]. The hypersharp nature of these boundaries is symptomatic of a polydisperse and highly nonideal (in the thermodynamic sense) system. Low speed sedimentation equilibrium in the analytical ultracentrifuge using Rayleigh interference optics and two different types of extrapo-*

Received January 22, 1996; accepted March 13, 1996.

* To whom correspondence should be addressed.

Biopolymers, Vol. 39, 729–736 (1996)

CCC 0006-3525/96/050729-08

lation procedure (involving point and whole-cell molar masses) gave a weight average molar mass M_w *of* $(2.5 \pm 0.5) \times 10^{-6}$ *g·mol*$^{-1}$ *and also a second virial coefficient,* $B = (2.8 \pm 0.7) \times 10^{-4}$ *mL·mol·g*$^{-2}$*, both values in good agreement with those from light scattering-based procedures (Part II of this series). A dynamic Zimm plot from dynamic light scattering measurements gave a z-average translational diffusion coefficient* $D^0_{20,w} = (3.02 \pm 0.05) \times 10^{-8}$ *cm*^{2}*·s*$^{-1}$ *and the concentration-dependence parameter* $k_D = (370 \pm 15)$ *mL/g. Combination of* $s^0_{20,w}$ *with* $D^0_{20,w}$ *via the Svedberg equation gave another estimate for* M_w *of* $\approx 2.4 \times 10^6$ *g/mol, again in good agreement. Both the Wales-van Holde ratio* ($k_s/[\eta]$) ≈ 0.4 *(with* $[\eta] = (760 \pm 77)$ *mL/g) and the ρ-parameter (ratio of the radius of gyration from static light scattering to the hydrodynamic radius from dynamic light scattering) as* $\rho > 2.0$ *all indicate an extended conformation for the macromolecules in solution. These findings, plus Rinde-type simulations of the sedimentation equilibrium data are all consistent with the interpretation in terms of a unimodal wormlike coil model performed earlier.* © *1996 John Wiley & Sons, Inc.*

INTRODUCTION

In previous papers of this series[1,2] the anionic polysaccharide known as xylinan was studied by static light scattering and viscometry. The measurements were performed in 0.10*M* NaCl on material that had been fractionated by gel permeation chromatography (Part I) as well as on the unfractionated parent sample at various ionic strengths (Part II). Results have given evidence for a semiflexible chain with a persistence length L_p as (100 ± 10) nm. The major proportion in solution consists of double-stranded chains (which are likely to be of the native form), but, dependent on the conditions upon isolation/preparation or the pretreatment of solutions, also single- and multistranded chains were found to be present in the chemically homogeneous population. Good solubility and the same overall structure were observed at ionic strengths ranging from 10 m*M* to 0.30*M* (adjusted by adding NaCl). The average molar mass for two somewhat differently prepared samples from the same broth (P1 and P2) was found to differ slightly with $M_w = 2.5 \times 10^6$ g/mol for P1 and $M_w = 1.9 \times 10^6$ g/mol for P2 (all measured in 0.10*M* NaCl). The corresponding thermodynamic second virial coefficients were determined as $B \approx 3.1 \times 10^{-4}$ mL·mol·g^{-2} and $B \approx 5.1 \times 10^{-4}$ mL·mol·g^{-2}, respectively. The possibility of a bimodal distribution as an alternative explanation to the wormlike coil distribution for the curvature of the scattering curves was ruled out on the basis of model calculations. However, to prove unequivocally the correctness of these conclusions it is necessary to resort to other independent absolute techniques, and this is the basis of the current investigation.

In this study we investigate further the homogeneity, average molar mass, and conformation of xylinan in aqueous, salt-containing solution using independent techniques such as analytical ultracentrifugation (sedimentation velocity and equilibrium), dynamic light scattering, and capillary viscometry. Specifically, we (i) use sedimentation velocity and sedimentation equilibrium in the analytical ultracentrifuge to check the homogeneity of the preparation, (ii) use sedimentation equilibrium and also "sedimentation-diffusion" (combination of the sedimentation coefficient from sedimentation velocity measurements with the translational diffusion coefficient from dynamic light scattering) to determine the average molar masses, and (iii) use the sedimentation coefficient concentration-dependence parameter k_s, the intrinsic viscosity $[\eta]$, the radius of gyration (from static light scattering), and the hydrodynamic radius (from dynamic light scattering) to make deductions about the conformation of the xylinan macromolecules in solution.

Like static light scattering measurements, dynamic light scattering requires sets of optically clean solutions of graduated concentration. Thus all details of clarification provided in Part II of this series are also relevant in this context. To prevent any ambiguity through variability of preparative effects, the same set of clarified solutions (sample P1) was used for all the following measurements, including the ultracentrifugation studies and viscometry. Further, the use of only a single ionic strength ($I = 0.10$ mol·L^{-1}) seems to be justified after our previous investigations have shown that, apart from B, the solution behavior is not significantly affected by the addition of salt.

EXPERIMENTAL

Preparation of Solutions

Solutions were prepared by dissolving the lyophilized polysaccharide directly into the solvent[1,2] to a maximum stock solution of ~ 2 mg/mL. Preparative ultracentrifu-

gation was performed on a Beckman L-5 centrifuge (~ 20°C; 1.5–2 h; 45,000 rev/min). The supernatant was separated from the precipitate by means of a syringe. The solution was filtered twice through a membrane filter of 0.45-μm pore size. The stock solution was diluted to give six concentration steps that were filtered subsequently through a 0.45-μm pore-size membrane into the measuring cells for the light scattering measurements (static and dynamic). They were taken afterwards for the ultracentrifuge studies and viscometry measurements. The polysaccharide concentration was determined by means of the phenol-sulfuric acid method related to glucose standards.

Ultracentrifuge Studies

Sedimentation Velocity Measurements. Sedimentation velocity experiments were performed in a Beckman (Palo Alto, U.S.A.) Model E analytical ultracentrifuge equipped with conventional phase-plate Schlieren optics, an LED light source,[3] and 12- or 30-mm (optical path length) single sector cells. A rotor speed of 40,000 rev/min and temperature of 20.0°C were employed. The sedimentation coefficients were corrected to standard conditions of solvent density and temperature (that of water at 20°C) in the usual way[4] to give $s_{20,w}$ values. The "infinite dilution" sedimentation coefficient $s^{\circ}_{20,w}$ was obtained from a conventional plot of $(1/s_{20,w})$ versus concentration c (corrected for radial dilution) and fitting to[5]

$$(1/s^{\circ}_{20,w}) = (1/s_{20,w})\{1 + k_s c\}$$

where k_s (mL/g) is the sedimentation concentration dependence regression coefficient.

Sedimentation Equilibrium Measurements. Sedimentation equilibrium experiments of the low speed type (to ensure optical registration of the pattern near the cell base) were performed using a different Model E analytical ultracentrifuge equipped with a 5-mW laser light source and a dedicated Rayleigh interference optical system. A rotor speed of 3000 rev/min at a temperature of 20.0°C was employed. Thirty-millimeter optical path length double sector cells were used at six loading concentrations in the range of ~ 0.2–1 mg/mL, respectively, with the dialysate in the reference channels. Short column lengths (1–2 mm) were also employed to enable equilibrium to be reached within ~ 1–2 days (for further details see Ref. 6). A partial specific volume $\bar{v}$ of 0.66 mL/g was employed, as measured in a density meter (Anton Paar, Austria).

Dynamic Light Scattering Measurements

The dynamic light scattering measurements were performed in cylindrical measuring cells using the instrument "Simultan" equipped with an ALV-5000 Multiple Tau Digital Correlator (ALV-Laser, FRG) and a 400-mW Nd-YAG laser light source (Adlas, FRG) with an operating wavelength of 532.8 nm. The measurements were carried out at 22°C in multiple sampling time mode. The autocorrelation functions were measured in homodyne mode in the angular range between 20 and 150° in steps of 10° each.

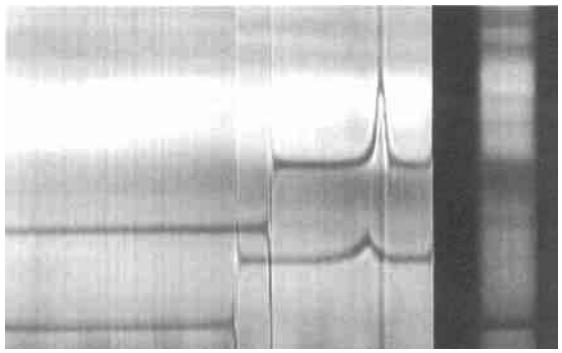

FIGURE 1 Sedimentation velocity Schlieren diagrams for unfractionated xylinan. Rotor speed = 40,000 rev/min, temperature = 20.0°C, solvent NaCl solution, I = 0.10. Top profile: loading concentration (corrected for radial dilution) 0.75 mg/mL. Bottom profile: 0.48 mg/mL. Top pattern displaced upwards for clarity using a wedged cell window. Note the single hypersharp boundary in each case, indicative of (i) sample purity and (ii) high thermodynamic nonideality.

Capillary Viscometry Measurements

An Ubbelohde-type capillary viscometer AVS 310 (Schott-Geräte, FRG) was used at 20.0°C. The intrinsic viscosity $[\eta]$ was obtained by plotting the reduced viscosity η_{red}/c versus c, the polymer concentration (linear regression to $c = 0$).

RESULTS AND DISCUSSION

Only single (Schlieren) peaks were observed from the sedimentation velocity records (Figure 1) confirming the unimodal nature of the preparation. These peaks are clearly hypersharp, characteristic of a polydisperse (in a quasi-continuous sense) but highly concentration-dependent (i.e., nonideal) system.[7] Similar hypersharp behavior was recently observed for the related xanthan molecule.[6] From a reciprocal plot of the sedimentation coefficient, $s_{20,w}$ versus concentration (corrected for radial dilution) c (Figure 2), a value for the infinite dilution sedimentation coefficient $s^{\circ}_{20,w} = (9.5 \pm 0.7)$ S and the concentration-dependence regression pa-

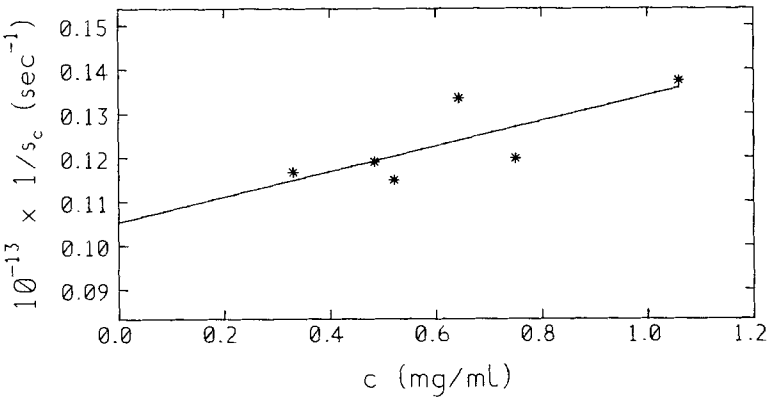

FIGURE 2 Concentration dependence of the reciprocal of the (apparent) sedimentation coefficient $1/s_{20,w}$. Concentrations are true sedimenting concentrations (i.e., corrected for moisture content and radial dilution). Line fitted is $1/s_{20,w} = (1/s^0_{20,w})\cdot(1 + k_s c)$.

rameter $k_s = (273 \pm 112)$ mL/g is obtained, indicating a very large nonideal molecule.

The sedimentation equilibrium measurements were used to produce an estimate for the apparent weight average molar mass $M_{w,app}$ corresponding to a series of cell loading concentrations c. The plot of the reciprocal apparent weight average molar mass versus cell loading concentration c is given in Figure 3. A linear fit was possible according to the equation[4]

$$(1/M_{w,app}) = (1/M_w) + 2Bc$$

to obtain an estimate of the "ideal" weight average molar mass M_w of $(2.5 \pm 0.5) \times 10^6$ ("whole cell" value) and the second thermodynamic virial coefficient $B = (2.8 \pm 0.7) \times 10^{-4}$ mL·mol·g^{-2}. A further estimate for M_w can be obtained by extrapolation of point average molar masses $M_{w,app}(r)$ to zero (fringe) concentration $J(r)$, possible with the longer solution column (2 mm) at the 0.27-mg/mL loading concentration (Figure 4). Graphical extrapolation to $J = 0$ yields an M_w of $\approx (2.7 \pm 0.5) \times 10^6$, where the error takes into account uncertainties in meniscus concentration evalua-

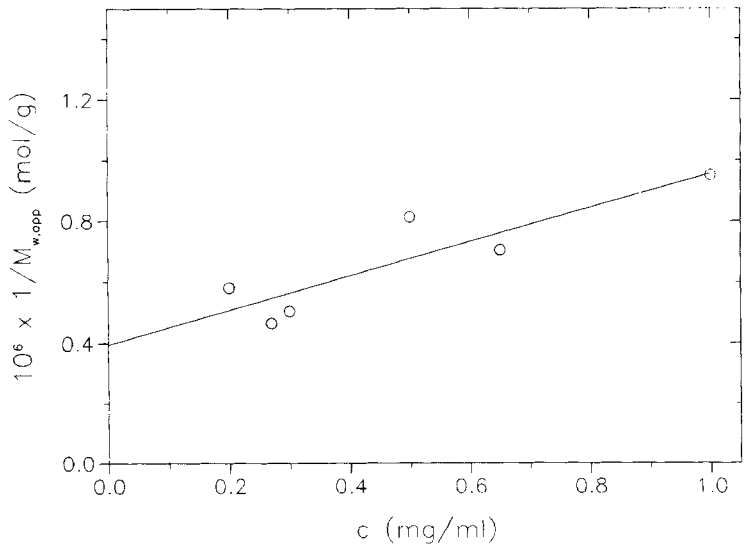

FIGURE 3 Concentration dependence of the reciprocal (whole-distribution) apparent weight average molar mass from low speed sedimentation equilibrium. The line fitted is to $(1/M_{w,app}) = (1/M_w) + 2Bc$ where B is the second thermodynamic or "osmotic pressure" virial coefficient.

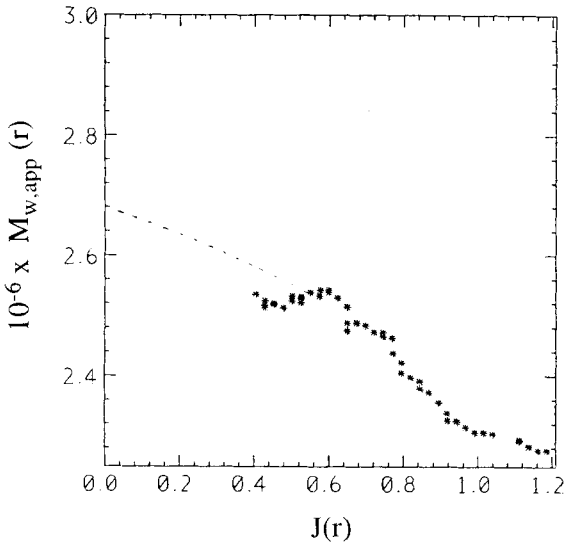

FIGURE 4 Plot of the point weight average molar mass $M_{w,app}(r)$ versus concentration [expressed as fringe displacement units $J(r)$]. Loading concentration $c = 1.0$ mg/mL, rotor speed = 3000 rev/min, temperature = 20.0°C.

tion.[8] Although this estimate involves a further approximation because of possible redistribution of material of species as a function of radial displacement, the result is consistent with the value from the conventional extrapolation of "whole-cell" values. Both values are in very good accordance with the weight average molar mass determined by static light scattering as $M_w = 2.5 \times 10^6$ g/mol. The B values from sedimentation equilibrium ($B \approx 2.8 \times 10^{-4}$ mL·mol·g^{-2}) and static light scattering ($B \approx 3.1 \times 10^{-4}$ mL·mol·g^{-2}) agree also very well.

A further estimate for the weight average molar mass is possible by use of the Svedberg equation (see, e.g., Ref. 4)

$$M_w = \{s^o_{20,w} \cdot RT\} / \{D^o_{20,w}(1 - \bar{v}\rho_{20,w})\}$$

with $\rho_{20,w}$ the density of water at 20°C and $D^o_{20,w}$ the translational diffusion coefficient (corrected to standard solvent conditions, viz. the temperature and viscosity of water at 20°C[4]). For polydisperse polysaccharide preparations, reliable values for the translational diffusion coefficient can be better obtained from dynamic light scattering measurements rather than from conventional boundary spreading experiments in the analytical ultracentrifuge.

The corresponding "dynamic Zimm plot" (see, e.g., Ref. 9) after a cumulant fit of third order is given in Figure 5. A double extrapolation to zero concentration and zero angle was performed to obtain a value for $D^o_{20,w}$ (z-averaged value) of (3.02 ± 0.05) × 10^{-8} cm^2·s^{-1}, and a value for the concentration-dependence parameter k_D of (370 ± 15) mL/g. It was shown[10] that a combination of the z-average translational diffusion coefficient with the (weight average) sedimentation coefficient yields the weight average molar mass. A value of $M_w \sim 2.4 \times 10^6$ g/mol is thus obtained, which is in

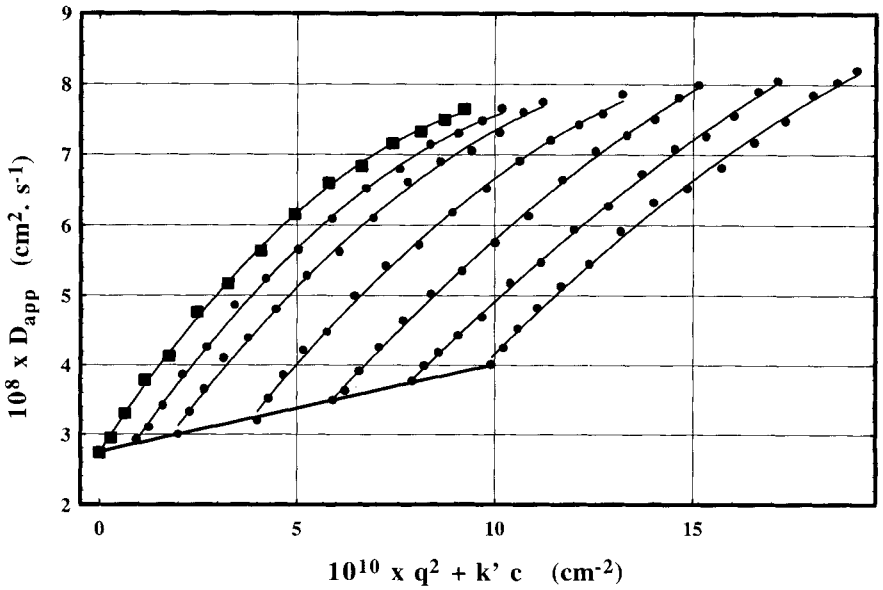

FIGURE 5 Dynamic Zimm plot of xylinan in 0.10M NaCl. q = Bragg wave vector.

Table I Hydrodynamic (and Thermodynamic) Parameters for (Unfractionated) Xylinan "P1"

Parameter	
M_w (g/mol) (sedimentation equilibrium, from $1/M_{w,app}$ extrap.)	$(2.5 \pm 0.5) \times 10^6$
M_w (g/mol) (sedimentation equilibrium, from $M_{w,app}$ (r) extrap.)	$(2.7 \pm 0.5) \times 10^6$
M_w (g/mol) (sedimentation diffusion)	2.4×10^6
M_w (g/mol) (static light scattering[1,2])	2.5×10^6
$s^0_{20,w}$ (S)	(9.5 ± 0.7)
k_s (ml/g)	273 ± 112
$D^0_{20,w}$ ($cm^2 \cdot s^{-1}$)	$(3.02 \pm 0.05) \times 10^{-8}$
k_D (ml/g)	370 ± 15
B ($ml \cdot mol \cdot g^{-2}$) (sedimentation equilibrium, from $1/M_{w,app}$ versus c data)	$(2.8 \pm 0.7) \times 10^{-4}$
B ($ml \cdot mol \cdot g^{-2}$) (static light scattering[1,2])	3.1×10^{-4}
$[\eta]$ (ml/g)	(769 ± 77)
Derived shape parameters:	
ρ ($=R_g/R_h$)	2.4
$k_s/[\eta]$	≈ 0.4
a/b	≈ 20

very good agreement with the values above from different approaches (Table I).

The translational diffusion coefficient D is related to the (z-average) hydrodynamic radius R_h according to the Stokes–Einstein relation (see, e.g., (Ref. 4))

$$R_h = kT/\{6\pi\eta_o D\}$$

with η_o the solvent viscosity for the temperature T and k is the Boltzmann constant. Consequently, the z-average R_h was calculated as $\sim$ 75 nm. This value combined with the z-average of the radius of gyration from static light scattering, R_g = 152 nm (Part II, Table, I) in terms of the ρ-parameter[9]

$$\rho = R_g/R_h$$

leads to $\rho > 2.0$, which is consistent with the worm-like chain conformation[11] inferred from Parts I and II of this series.

An idea of the conformation of the xylinan molecules can be additionally obtained from the ratio of $k_s/[\eta]$ originally given by Wales and van Holde[12] and which has a value of $\sim$ 1.6 for spheres and random coils and $\sim$ 0.2 for rigid extended structures.[13] Thus, from our values of $[\eta]$ = (769 $\pm$ 77) mL/g and k_s = (273 $\pm$ 112) mL/g we can conclude from the corresponding value of $k_s/[\eta] \approx 0.4$ that the xylinan molecules approach extended rod behavior. Further use can be made of this ratio; if we approximate the molecule by the equivalent hydrodynamic rigid prolate ellipsoid, we can estimate the shape independent of any assumed value for the hydration,[13–15] and from simple inversion formulas giving the aspect ratio a/b (ratio of semimajor axis a to semiminor axis b) as a function of $k_s/[\eta]$[16] an a/b of the order of $\approx$ 20 can be predicted.

Although all the results so far have been found to be consistent with the interpretation in terms of a homologous polymer series, it would still be instructive to examine the possible existence of a bimodal system (since this seems to be a characteristic feature of several related polysaccharide systems, even after appropriate filtration) even though this was refuted on the basis of model calculations performed in Part II of this series on the static light scattering data. Similar calculations can be performed on the sedimentation equilibrium data in this study by performing Rinde-type[17,18] simulations of the concentration distributions for noninteracting mixtures in terms of (i) a two-component model (making use of the parameters that were initially considered as a possibility from static light scattering, before being rejected) and (ii) a one-component model. Because of the complex nature of the theory and considerable demands on computer resources, simulations of the full nonideal Rinde type are not possibly for species of widely different molar mass.[19] Instead we take the equilibrium concentration distribution data from a very low loading concentration (0.3 mg/mL) to minimize nonideality complications and make the approximation of using apparent molar masses inserted into the ideal Rinde equations where the concentration distribution for each component i of an ideal noninteracting n-component mixture is given by

$$J_i(r) = J_i^o\left\{\frac{A_i(b^2 - a^2)\exp[A_i(r^2 - a^2)]}{\exp[A_i(b^2 - a^2)] - 1}\right\}.$$

where the A_i are the reduced molar masses $\{(1 - v\rho_o)\omega^2/(2RT)\} \cdot M_i$, ω is the angular velocity, a and b the radial positions at the meniscus and cell base, respectively. The J_i^o is the initial cell loading

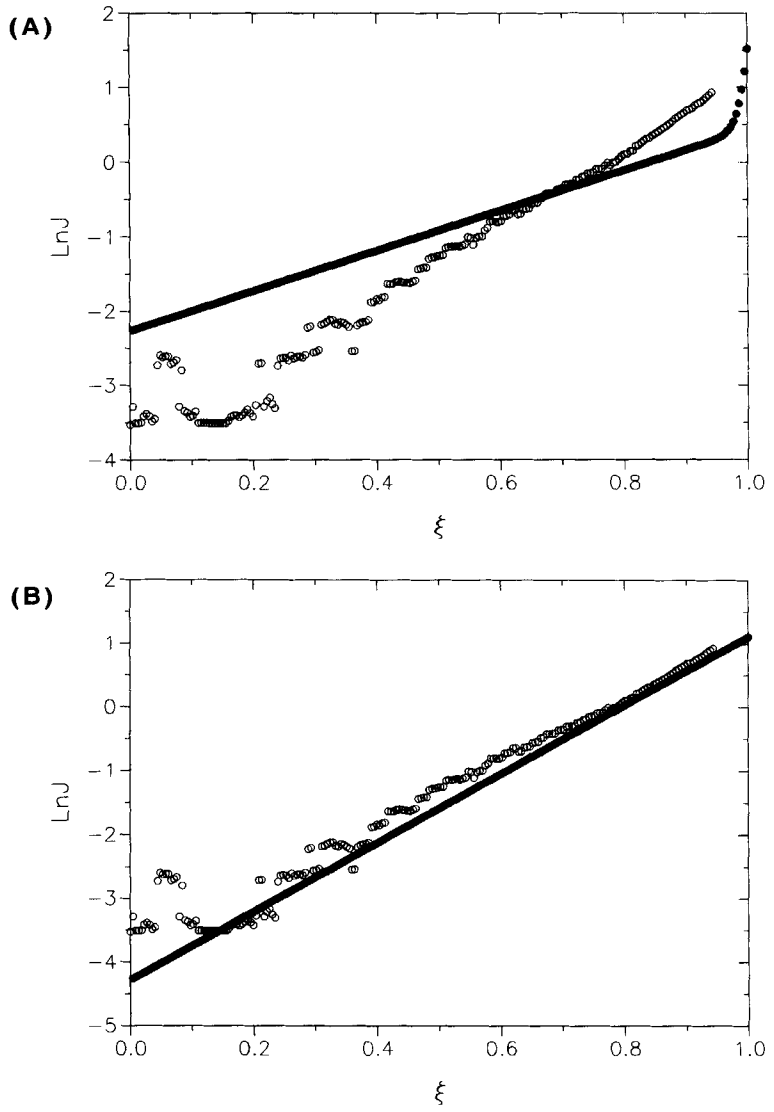

FIGURE 6 Rinde-type simulations of the concentration distribution from sedimentation equilibrium. (a) Two-component system (95% $M_{app} = 2 \times 10^6$ g/mol; 5% $M_{app} = 40 \times 10^6$ g/mol). (b) One-component system ($M_{app} = 2 \times 10^6$ g/mol). Experimental data (open circles) from loading concentration = 0.3 mg/mL, rotor speed = 3000 rev/min, temperature = 20.0°C. Simulated data: filled circles (200 data points). J: concentration at a given radial displacement r. ξ: normalized radial displacement squared parameter $[=(r^2 - a^2)/(b^2 - a^2)]$ where a, b = radial positions at the meniscus and cell base respectively.

concentration for a given component. The total concentration is therefore $J^o = \Sigma_i J_i^o$. The total concentration at each radial point in the cell is $J(r) = \Sigma_i J_i(r)$. Figure 6a shows the simulation (200-data point fit) for a two-component mixture, with the 0.3-mg/mL loading concentration made up of 95% of species of apparent molar mass 1×10^6 g/mol and 5% at 40×10^6 g/mol. Even though the apparent weight average mass of this mixture is as high as 3×10^6 g/mol the fit is clearly too shallow. The trend in the data is, however, faithfully reproduced for a single-component fit of $M_{app} = 2 \times 10^6$ (the measured apparent molar mass) (Figure 6b). This disproves the contribution of any supramolecular component to the average apparent molar masses determined by sedimentation equilibrium performed at a low rotor speed (3000 rev/min). As already stated, no supramolecular component was observed in the sedimentation velocity optical records.

In conclusion, the self-consistency of all data from a variety of techniques gives the results and their interpretation in terms of double-stranded stiff chains, with a persistence length of ~ 100 nm as the most likely conformation in aqueous systems, a high level of confidence. The close relationship between xylinan and xanthan not only by chemical structure but also by conformation has also become apparent (cf., Refs. 1, 2, 6, and 20, although the current series of papers makes no comment on any order/disorder transition behavior). The combination of hydrodynamic techniques (analytical ultracentrifugation, dynamic light scattering, and viscometry) with static light scattering—standing alone or in combination with gel permeation chromatography—has shown to be a useful strategy for the macromolecular characterization of the chemically homogeneous but complex polysaccharide xylinan.

This work was supported by the Commission of the European Communities (Human Capital & Mobility Programme, Contract ERBCHBGCT921040) and the Biomolecular Sciences Committee of the United Kingdom BBSRC/EPSRC.

REFERENCES

1. Berth, G., Dautzenberg, H., Christensen, B. E., Rother, G. & Smidsrød, O. (1996) *Biopolymers* **39,** 709–719.
2. Berth, G., Dautzenberg, H., Christrensen, B. E. & Smidsrød, O. (1996) *Biopolymers* **39,** 721–728.
3. Cölfen, H., Husbands, P. & Harding, S. E. (1995) *Prog. Coll. Int. Sci.* **99,** 194–199.
4. Tanford, C. (1961) in *Physical Chemistry of Macromolecules,* John Wiley and Sons, New York, NY, Chapters 5 and 6.
5. Schachman, H. K. (1959) *Ultracentrifugation in Biochemistry,* Academic, New York, NY.
6. Dhami, R., Harding, S. E., Jones, T., Hughes, T., Mitchell, J. R. & To, K. M. (1995) *Carbohydr. Polym.* **27,** 93–99.
7. Peacocke, A. R. & Schachman, H. K. (1954) *Biochim. Biophys. Acta* **15,** 198.
8. Creeth, J. M. & Harding, S. E. (1982) *J. Biochem. Biophys. Methods* **7,** 25–34.
9. Burchard, W. (1988) *Macromol. Chem. Macromol. Symp.* **18,** 1–5.
10. Pusey, P. N. (1974) in *Photon Correlation and Light Beating Spectroscopy* Plenum, NY, p. 387.
11. Burchard, W. (1992) in *Laser Light Scattering in Biochemistry,* Harding, S. E., Sattelle, D. B., and Bloomfield, V. A., Eds., Royal Society of Chemistry, Cambridge, UK, Chapter 1.
12. Wales, M. & van Holde, K. E. (1954) *J. Polym. Sci.* **14,** 81–86.
13. Rowe, A. J. (1977) *Biopolymers* **16,** 2595–2611.
14. Creeth, J. M. & Knight, C. G. (1965) *Biochim. Biophys. Acta* **102,** 549–558.
15. Lavrenko, P. N., Linow, K. J. & Görnitz, E. (1992) in *Analytical Ultracentrifugation in Biochemistry and Polymer Science,* S. E. Harding, A. J. Rowe, and J. C. Horton, Eds., Royal Society of Chemistry, Cambridge, UK, pp. 394–406.
16. Harding, S. E. & Cölfen, H. (1995) *Anal. Biochem.* **228,** 131–142.
17. Rinde, H. (1928) PhD Thesis, Uppsala, Sweden.
18. Fujita, H. (1962) *Mathematical Theory of Sedimentation Analysis,* Academic Press, New York, NY.
19. Harding, S. E. (1985) *Biophys. J.* **47,** 247–250.
20. Berth, G., Dautzenberg, H., Christensen, B. E., Harding, S. E., Rother, G. & Smidsrød, O. (1996) *Macromolecules* **29,** 3491–3498.